OPEN ACCESS

GAVIN PUBLISHERS

Nanomedicine and Nanoscience Research

Research Article

Felipe RF, et al. J Nanomed Nanosci: JNAN-156.

DOI: 10.29011/2577-1477.100056

Molecular Junction based on ZigZag Silicene Planar NanoRibbon (ZZ-SiPNR): Density Functional Theory (DFT) and Extended Hückel Theory / Non-Equilibrium Green Function (EHT/NEGF)

Rafaela Farinha Felipe[1], Kazuko Ramos Nisioka[1], Jordan Del Nero[2*], Vicente Ferrer Pureza Aleixo[3], Carlos Alberto Brito da Silva Jr[3]

[1]Faculty of Materials Engineering, Federal University of Pará, PA, Brazil

[2]Faculty of Physics, Federal University of Pará, 66075-110 Belém, PA, Brazil

[3]Faculty of Physics, Federal University of Pará, 67113-901 Ananindeua, PA, Brazil

[*]**Corresponding author:** Jordan Del Nero, Faculty of Physics, Federal University of Pará, 66075-110 Belém, PA, Brazil. Tel: +55-9132017423; Email: jordan@ufpa.br

Citation: Felipe RF, Nisioka KR, Nero JD, Aleixo VFP, Jr. Silva CABD (2018) Molecular Junction based on ZigZag Silicene Planar NanoRibbon (ZZSiPNR): Density Functional Theory (DFT) and Extended Hückel Theory / Non-Equilibrium Green Function (EHT/NEGF). J Nanomed Nanosci: JNAN-156. DOI: 10.29011/2577-1477.100056

Received Date: 06 November, 2018; **Accepted Date:** 30 November, 2018; **Published Date:** 07 December, 2018

Abstract

In this work we propose an investigation of the electronic transport properties of a Molecular Junction (MJ) composed by ZigZag Silicene Planar NanoRibbon (ZZSiPNR) by means of Density Functional Theory (DFT) on the Unit Cell (UC) and Extended Hückel Theory / Non-Equilibrium Green Function (EHT/NEGF) using the Landauer-Buttiker formule for ZZSiPNR coupled to two Leads of the same chemical species forming the MJ. Our results exhibit Topological Insulator (TI) behavior due the valence and conduction bands pass an odd number of times (five times) by ε_F for the UC at zero bias, while for the MJ a non-linear region characteristic of a Negative Differential Resistance (NDR) at $V_e = 1.7V$ emerge in the I-V_e curve characterizing an electronic nanodevice, Resonant Tunnel Diode-Like, RTD-Like. This non-linear voltage region coincides with the minima voltage (V_{min}) in the Fowler-Nordheim (FN) and Lauritsen-Millikan (LM) plots for MJ of ZZSiPNR by Transition-Voltage Spectroscopy (TVS) analysis.

Keywords: Nanodevice; Nanoribbon; Silicene

Introduction

The Silicon (Si), which in Latin means “Hard Rock”, is a chemical element that belongs to group 14 of IV A family of the Periodic Table with atomic number 14 (14 protons and 14 electrons) and atomic mass 28, with an electronic distribution ($1s^2$, $2s^2$, $2p^6$, $3s^2$ and $3p^2$) presenting 4 valence electrons in the semi-filled sp sub-levels at the third energy level (M layer). Its properties are intermediate between those of carbon (C) and germanium (Ge). At room temperature, Si is in the solid state in the form of a brown powder (amorphous) more reactive than the crystalline form to which is a very hard and poorly soluble octahedron of greyish blue and metallic luster. It was discovered by Swedish chemist J.J. Berzelius (1779-1848) in 1823 and is the second most abundant element (28%) in the earth’s crust, as it is an essential component of most rocks, such as clay, feldspar, granite, quartz and sand, usually in the form of silica or Si dioxide (SiO_2) and silicates (compounds containing Si, O and metals). Si is the main component of glass, cement, ceramics (porcelain), most semiconductor components and silicones. It is used for the production of metallic alloys, and because it is a very abundant semiconductor material. The band structure of Si is very well-known: an indirect gap semiconductor of 1.1eV at room temperature and with valleys approximated by quadratic dispersions. It has a special interest in the manufacture of optical waveguides due to its high refractive index (3.5 which transmits infrared radiation) and in the electronics and microelectronics industry, as basic material for the production of transistors for chips, solar cells and others [1,2].

For medicine the Si is one essential oligoelement (substance of mineral origin, better known as biocatalyst) that is present in the human organism in small traces, in small amounts as the name

suggests (oligo means little) involved in tissue reconstitution. High concentrations of Si are located in connective tissue responsible for establishing and keep body shape and connect others tissue. Hard tissues as tendons, cartilages, trachea, cornea, nails, skin, hair and arteries contain significant amounts of Si [3]. Absence of that substance can cause changes in bones and cartilages, difficulties in consolidating fractures, loss of vascular elasticity, hair loss and diseases cutaneous [4,5]. Si derivatives such as SiO_2 are useful to combat low back pain, the application triggers biological effects causing improves lumbar analgesia, acceleration of enzymatic reactions and activation of blood and lymphatic circulation [6,7]. In the past two decades, researchers have driven their attention to the investigation of the electronic transport properties of Two-Dimensional (2-D) materials with only one atom of thickness in the layer [8]. The discovery of graphene led to an increase in the exploration of these 2-D materials [9,10], such as Silicene [11-15], Germanene [16], Phosphorene [17,18], Stanene [19], hexagonal Boron Nitride (h-BN) known as white graphite [20], and Transition Metal Dichalcogenides (TMDs) [21] for Nanoelectronics, Optoelectronics and Thermoelectric [9,10].

The Si graphene equivalent was first mentioned in a theoretical study by Takeda and Shiraishi [11] in 1994 and then reinvestigated by Guzman-Verri and L.C. Lew [12] in 2007, who named it as silicene. The synthesis of this material occurred around 2010 by B. Lalmi, et al. [13] and B. Aufray, et al. [14] and 2012 by P. Vogt, et al. [15]. With this, it was possible to predict that silicene is a kind of "Si graphene" formed by a hexagonal monolayer of Si atoms with sp^2-sp^3 mixed hybridization leads to a buckled structure, e, distinguishing silicene from the planar graphene (C-C = 1.42Å), which brings with it the promise of a new wave of miniaturization and faster electronic equipment with less energy consumption. The advantage of using silicene is that it is naturally semiconducting like Si, which is the basis of all electronics, which places it as a material capable of replacing Si directly, but is ultra-fine like graphene. Compared with graphene, silicene is more compatible with Si-based semiconductor devices and the present silicon Complementary Metal-Oxide-Semiconductor (CMOS) technology in comparison to graphene and thus has greater potential in nanoelectronic applications. However, in spite of its exceptional electrical and electronic properties, working with silicene is very difficult because, unlike graphene, which is stable and flat, the monoatomic layer of Si has "Relief", with the Si atoms remaining under tension, furthermore, it does not exist in nature and can only be produced in the laboratory which is very difficult. This explains why little progress has been made in the area since the silicene was isolated in 2012 [11-15].

The band structure of 2-D silicene (in the absence of spin orbit interaction) has a zero gap at the ε_F, together with the valence and conduction bands crossing with linear dispersions, so-called Dirac cones; these occur at the K and K´ points in the hexagonal Brillouin Zone (BZ) forming valleys, and the two degenerate bands at a given point originate from the A and B sublattices of the silicene structure. Due to the absence of mirror symmetry, p_z states are coupled to p_x and p_y states, as well as s states in forming the states near the ε_F. Inclusion of spin-orbit coupling would open a small gap of 1.55meV. Silicene is similar to graphene in being a Kane-Mele type 2-D Topological Insulator (TI) but of course differs from Si which is a band insulator (BI). A 2-D TI has a bulk energy gap but gapless edge states that allow correlated charge and spin transport. Nevertheless, silicene is also different from graphene in that the buckled structure allows for more topological phases.

However, application in Field Effect Transistors (FETs) requires a band gap of more than 0.4eV to achieve an adequate switching behavior. In order to, overcome these disadvantages, and modulate the bandgap of 2-D Silicene, we use hydrogenation of the inferior and superior edges of the zigzag configuration (H atoms bonded with Si atoms to make the system more stable) to form the 1-D ZigZag Silicene NanoRibbon (ZZSiNR).The ZZSiNR band gap decreases with increasing width (W) and can be tuned by apply an external electric field, where the π electrons responsible for the top of the valence band and bottom of the conduction band accumulate at different edges of the nanoribbon, especially in the narrow case. A FET based on ZZSiNR (N = 6) has been predicted to have a band gap of 0.44eV. A band gap of 0.45eV is predicted for silicene decorated with alkali metal atoms. Silicene nanoribbon can be used to realize a field-effect topological quantum transistor due to the quantized conductance changing from 2 to 0 in an electric field [2].

In this sense, we decided to investigate the electronic transport properties and Transition-Voltage Spectroscopy (TVS) of Molecular Junction (MJ) composed by ZigZag Silicene Planar NanoRibbon, ZZSiPNR (2,2), see (Figure 1), using the Density Functional Theory (DFT) to optimize the geometry of the unit cell of the molecule and the Extended Hückel Theory / Non-Equilibrium Green Function (EHT/NEGF) for the calculation of the electronic transport of ZZSiPNR (2,2) junction [22,23]. The TVS [24] is treated by means of the coherent molecular transport model since the electronic transport occurs by discrete occupied molecular levels in regions where V_{min} is located in the Fowler-Nordheim plots [FN or ln (I/V^2) x $1/V_e$] and Lauritsen-Millikan [LM or ln (I) x $1/V_e$] [25,26], as well as the possibility for nanoelectronic applications.

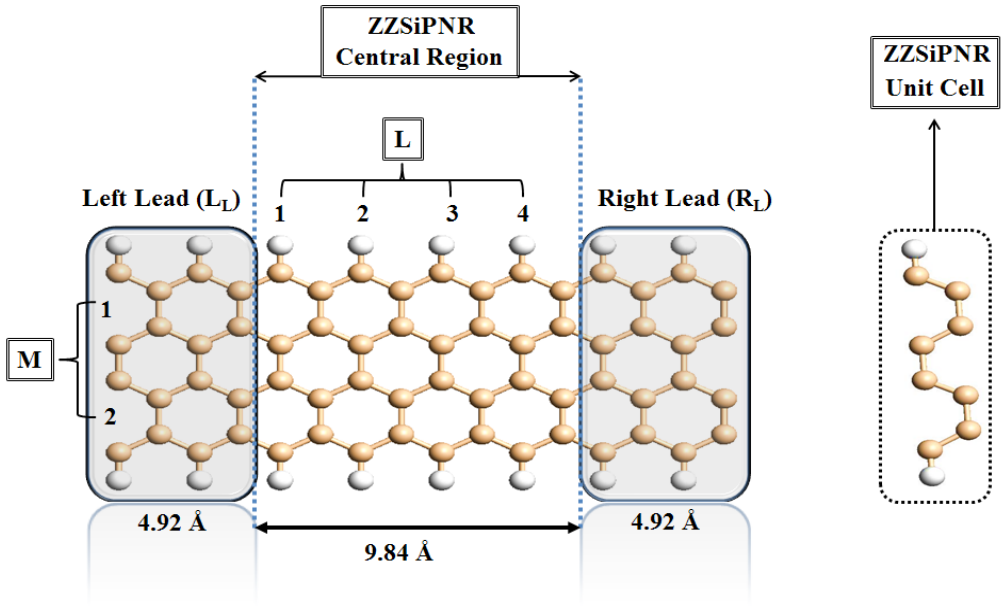

Figure 1: ZZSiPNR Structure. The Hamada index (2,2).

Material and Methods

The DFT formalism is highly reliable for optimizing geometry and describing electronic properties of single molecules [27-29]. Then, we chose the Unit Cell (UC) for the crystalline structure of ZZSiPNR that we treated as bulk and applied DFT-based calculations with Exchange-Correlation (XC) potential of the Local Density Approximation (LDA) with Perdew-Zunger (PZ) parametrization, [30], i.e., *LDA.PZ*. The base set for the Linear Combination of Atomic Orbital (LCAO) chosen was Double-Zeta Polarized (DZP) for the Si atoms as well as the parameters of the iteration (energy cut-off for the electrostatic potentials = 200 Ry, tolerance = 4.10^{-5} and maximum step = 200) while the first Brillouin Zone (BZ) was defined with k-points (1x1x100) and periodic boundary conditions were applied to determine the electronic properties (band structure, DOS and Transmittance). The structures are relaxed until the atoms forces converge to 0.02 eV/Å. On the other hand, DFT calculations are computationally non-viable for systems with more than 200 atoms.

For this reason, we take the optimized geometry (that is, the coordinates of all the atoms and the defined unit cell) that will be used to calculate the electron transport [T (E, V)] and TVS of the molecular junction attacked by Leads), which has been applied to the molecular conduction [26], where the electronic structure is calculated using a model with parameters adjustable to experiments and that combined with the technique of the Non-Equilibrium Green´s Function (NEGF) to determine quantum transport [29,31,32] under the effect of external voltage and that when used within their limitations generate very precise results. However, the main advantage of this method is the low computational cost, but it captures most of the electronic and atomic structure effects. Using the EHT, systems with up to 1000 atoms can be simulated easily [23]. The EHT is formulated in terms of the small set of Slater atomic orbitals $\{|\varphi_i>\}$, its overlaps $\{S_{ij}=<\varphi_i|\varphi_j>\}$ and a Hamiltonian matrix $\{H_{ij}=<\varphi_i|H|\varphi_j>\}$, where the elements of the diagonal matrix $H_{ii}=\varepsilon_I$ are the ionization energies of the experimentally determined atomic orbitals and the other elements of this matrix have the form defined by Ammeter et al. by consistency with the data of the experimental molecular electronic structure. However, the S_{ij} and H_{ij} used in the calculations have the plane wave form in the reciprocal k-space. Therefore, the Schrödinger equation EHT can be solved [33].

For electronic transport calculations, we must specify the Leads (Left and Right) and the central/scattering region, where the Leads must be periodic and correspond to the repetition of the scattering region of the unit cell in the z direction, which is the direction of electronic transport. Hamiltonian matrices are constructed for the two Leads of the standard EHT calculations on the periodic bulk device for the semi-infinite region. The temperature of the electrons is 300K. At the beginning of the calculations, the molecule relaxes freely with the application of external bias voltage (V_e) and a structural rearrangement of the complete junction occurs as a result of the EHT calculation optimization process. Thus, the basic structure for the device is based on ZZSiPNR which can be seen in (Figure 1), where the electronic transport will be calculated. In this step, the calculations are made with EHT and the input parameters are defined by configuring the EHT with the Hoffmann

parameters and we perform a consistent calculation to obtain the transmission spectrum because the transmittance is dependent of k for a given energy.

Now we can calculate the electric current (I-V_e curve) by applying a finite external bias voltage (V_e) between the electrodes for the ZZSiPNR device. For this, we apply the NEGF technique, because the transmittance for each voltage, T (E, V_e), is calculated after the molecular relaxation when applying V_e ranging from 0V to 3V for the direct and reverse bias between the Leads. Thus, it is then possible to calculate the central region / scattering current of a system with two electrodes for each voltage applied by means of the Landauer-Büttiker formula (see Eq.1 bellow) [34,35].

$$I = \frac{2e}{h}\int_{u_L(V_e)}^{u_R(V_e)} T(E,V_e)dE \qquad (1)$$

Where $u_L(V_e)$ and $u_R(V_e)$ are the energy polarization regions of the Leads, Left (L) and Right (R), respectively. T (E, V_e) is the transmission coefficient as a function of the electronic energy E under V_e which is given by Eq. (2) below

$$T(E,V_e) = tr\left[\Gamma_1^L G_C \Gamma_2^R G_C^*\right] = tr\left[\Gamma_1^L A_2^R\right] = tr\left[\Gamma_2^R A_1^L\right] \quad (2)$$

Where G_C and G_C^+ are the functions of delayed and advanced Green of the central region (channel), $\Gamma_{1/2}^{L/R} = i\left[\sum_{L/R} - \sum_{L/R}^*\right]$ is the tunneling rate between the molecular level (E_i) and the Leads (L and R) or "Enlargement" functions that are responsible for transport of the electrons in the system and by the amplification of the levels, since they take into account the coupling of the channel (molecule or central region / spreading) with the leads, $\sum_i^{L/R} = t_{L/R} g_{L/R} t_{L/R}^*$ is the function or matrix of auto energy of the leads, $g_{L/R} = (E - H_{L/R})^{-1}$ is the Green function of the electrodes and $t_{E/D}$ is the Hamiltonian coupling of the leads in the molecule and $A_{1/2}^{L/R}$ are the partial spectral functions of the left and right leads.

Results and Discussion

The hexagonal configuration of planar is obtained by the Hamada index specified by the integers (M, N) and used to obtain the structure of the planar silicate with sp^2 hybridization containing the hydrogenated edges that is re-optimized to form the ZZSiPNR. The UC of ZZSiPNR is composed of 8Si and 2H. The central/spreading region of the ZZSiPNR molecular junction is composed of 4 replicates of the UC, i.e., 32Si and 8H. By coupling the central/scattering region to the Leads (Left and Right) which are also each composed of two UC (i.e., 16Si and 4H), we have the Molecular Junction (MJ) of ZZSiPNR effectively. We consider as a starting point in the construction separately of the central region of the molecular junction of ZZSiPNR rectangular with width = W (chain number in the armchair direction) and length = L (chains number in the zigzag direction). Thus we define Hamada index (M = N = 2) for the chains number in the armchair direction through the nanoribbon and we specify the parameters (W = 2 and L = 4) which the W parameter define the SiPNR type because is related with the Hamada indices (M, N) characterizing the ZZSiPNR (2,2) [36]. The Hamada index defines the zigzag nature and metallic behavior of these nearly 2-D Dirac materials. When we coupled the Leads (Left and Right) which correspond to the repetition of the ZZSiPNR (2,2) unit cell of central/scattering region in the z direction which is the direction of the electronic transport to form the MJ or a device configuration with the dimensions determined in (Figure 1).

The average bond lengths for ZZSiPNR (2,2) are Si-Si ≅ 2.21Å and Si-H ≅ 1.46Å. The central region of the ZZSiPNR (2,2) was optimized by DFT/B3LYP/6-311G and the electronic properties of the UC of ZZSiPNR (2,2) was calculated by DFT/LDA.PZ/DPZ with length of 9.84Å. The Molecular Junction (MJ) is composed of the central region coupled to the Left Lead (LL) and Right Lead (RL) where the electronic transport was calculated by EHT/NEGF. The Leads correspond to two repetitions of the UC and has length of ≅ 4.92Å, while the central/scattering region corresponds to four repetitions of the UC for ZZSiPNR (2,2). The (Table 1) shows the results of the geometry optimization by DFT/B3LYP/6-311G (d, p) calculation for the energy of the Frontier Molecular Orbital (HOMO-2 to LUMO + 2) of the central region of MJ. The bandgap is determined by $E_{gap} = E_{LUMO} - E_{HOMO}$ which is equal to 0.132eV characterizing a TI behavior of the ZZSiPNR (2,2).

FMO	Energy for ZZSiPNR (2,2)
HOMO-2	-4.43052eV
HOMO-1	-4.32237eV
HOMO	-4.19685eV
LUMO	-4.06503eV
LUMO+1	-3.67646eV
LUMO+2	-3.63591eV

Table 1: The Frontier Molecular Orbitals (FMOs) via DFT/B3LYP/6-311G (d, p) calculation, where the $E_{gap} = E_{LUMO} - E_{HOMO} = 0.132$eV.

When silicene is modeled on a nanoribbon of One Dimension (1-D), there are quantization effects dictated by the set boundary conditions, which may result in: (1) Van Hove singularities at the k-points (ZZSiPNR hexagon vertex) for the Density of States (DOS) that only depends on the energy and (2) a bandgap depending on chirality and width. (Figure 2) exhibits the electronic properties of ZZSiPNR as bulk based on the investigation of its unit cell (UC) in which we determine the band structure, DOS and transmittance in V = 0V via DFT with LDA.PZ functional and DZP base set [37].

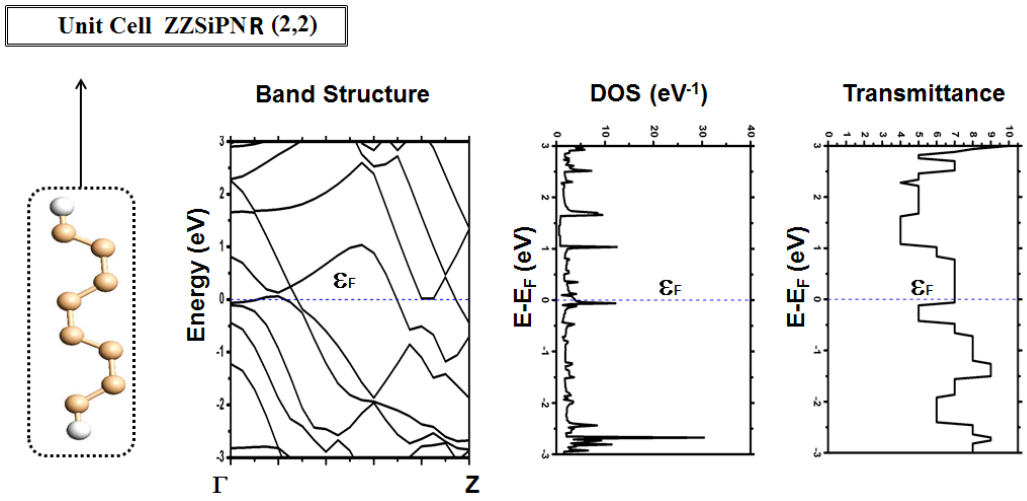

Figure 2: Electronic properties determined on the Unit Cell (UC) of ZZSiPNR (2,2) by DFT/LDA.PZ/DZP, where the bands near the Fermi level (ε_F) are due to edge states.

The band structure and DOS show that this material is a topological insulator (TI because has a band gap very small) due the valence and conduction bands pass an odd number of times (five times) by ε_F for the UC at zero bias in the ZZSiPNR (2,2). The DOS exhibits Van Hove singularities which is characteristic of almost 1-D materials where the Si atoms in the ZZSiPNR are located. The $\varepsilon_F \approx$ -4.35 eV, but it was centered at 0eV [38]. The transmittance exhibits transmission peaks in the ε_F and in the allowed regions of the valence and conduction bands. The calculations converged at 13 steps with tolerance of $\approx 2.41 \times 10^{-5}$.

Subsequently, we coupled the Leads (Left and Right) of same chemical specie in ZZSiPNR (2,2) to effectively construct the ZZSiPNR (2,2) devices (or molecular junction) using EHT with the Hückel base set of the Hoffmann type for Si and H for the calculation of DOS and Transmittance in V_e = 0V, obtaining the same values of the UC. The ε_F is approximately -7.6eV, while the chemical potential of the Leads (L and R) is approximately -6.24eV and -7.6eV for the ZZSiPNR (2,2) devices. The DOS at V_e = 0V show that they are TI because they have a peak at the Fermi level ($\varepsilon_F = E\text{-}E_F = 0$) because the conduction (LUMOs) and valence (HOMOs) energy levels pass this point. Transmittance exhibits transmission peaks at the ε_F and in the permitted regions (valence and conduction). The calculations converged in 15 steps with tolerance of $\approx 3.93 \times 10^{-5}$.

(Figure 3) shows the electronic transport properties of the molecular junction by means of EHT/NEGF calculations through current-voltage (I-V_e) and conductance-voltage (G-V_e) curves, and the Fowler-Nordheim (FN) and Lauritsen-Millikan (LM) for voltage range of -3V to + 3V [39,40].

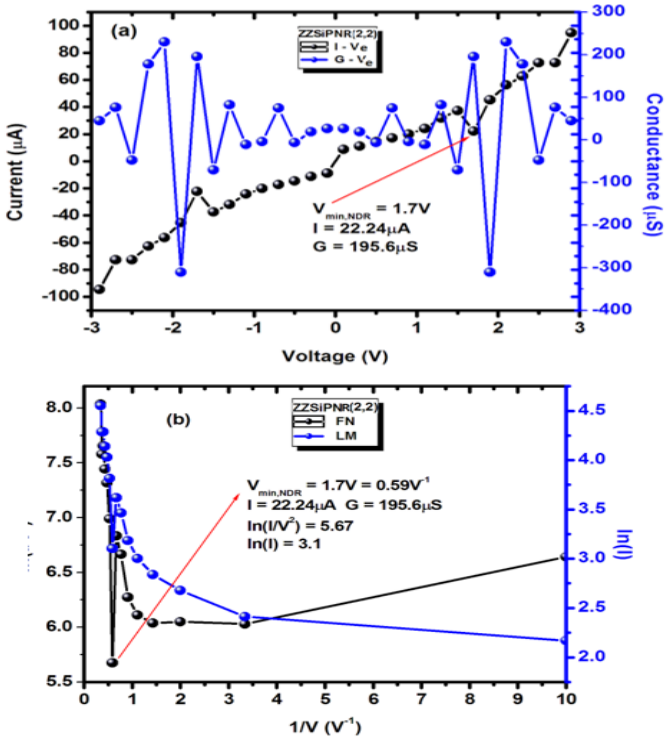

Figure 3: Electronic transport of junctions determined by means of EHT/NEGF calculations. (a) We show the I-V_e and G-V_e curves and the (b) FN and LM Plots. The red arrow in I-V_e and G-V_e curves show points where resonance and NDR on the voltage scale occur. These points coincide with the inflection points in the FN and LM plots. Calculations converged in 18 steps with tolerance of approximately 2.17×10^{-5}.

Therefore, we identify for ZZSiPNR (2,2) junction: A Negative Differential Resonance (NDR) at 1.7V ($0.59V^{-1}$), where the current value is 21.33μA. This voltage point where the NDR occurs corresponds to the minimum voltage, V_{min}, in the plots FN and LM. The V_{min} corresponds to the point in the FN plot equal to 5.7 and LM plot equal to 3.09. The maximum current is I_{max} = 94.64μA at 2.9V. Thus, we observed that the behavior of the I-V_e curve is characteristic of a Resonant Tunnel Diode (RTD). The origin of the NDR is due to the alignment of the Fermi level of the Lead (ε_F) with the energy of the LUMO, that is, $\varepsilon_F = E_{LUMO}$.

Conclusion

In this work, we investigated via DFT and EHT/NEGF calculations the electronic transport properties of molecular junction based on ZZSiPNR (2,2). The results show TI behavior, high electrical conductivity (high current, I_{max} = 94.64μA at 2.9V) where a TI-metal transition may occur and characteristic of a RTD due a NDR appears at V_e = 1.7V, i.e., a suppression of the current in this point ($I_{1.7V}$ = 21.33μA) in the I-V_e curve. The V_{NDR} correspond to V_{min}, i. e., $V_{NDR} = V_{min}$ = 1.7V ($0.59V^{-1}$) in the TVS analysis by means of FN and LM plots.

Acknowledgments

The authors acknowledge financial support from CNPq.

References

1. Wisniak J (2000) Jöns Jacob Berzelius a Guide to the Perplexed Chemist. Chem Educator 5: 343-350.
2. Lew Yan Voon LC, Zhu J, Schwingenschlögl U (2016) Silicene: Recent theoretical advances. Appl Phys Rev 3: 040802.
3. Carlisle EM (1982) The Nutritional Essentiality of Silicon. Nutr Rev 40: 193-198.
4. Féron JM (2014) Fracture consolidation and osteoporosis. Medicographia 36: 156-162.
5. Weiss RM (2007) Lasting Effects of Lost Vascular Elasticity. Circ Res 100: 604-606.
6. Gohel M, Patel M, Amin A, Agrawal R, Dave R, et al. (2004) Formulation Design and Optimization of Mouth Dissolve Tablets of Nimesulide Using Vacuum Drying Technique. AAPS Pharm Sci Tech 5: e36.
7. Chung Y, Chien H, Chen H, Yeh M (2014) Acupoint Stimulation to Improve Analgesia Quality for Lumbar Spine Surgical Patients. Pain Manag Nurs 15: 738-747.
8. Dresselhaus M S (2012) Fifty years in studying carbon-based Materials, Phys. Scr T146: 014002.
9. Novoselov KS, Geim AK, Morozov SV, Jiang D, Zhang Y, et al. (2004) Electric Field Effect in Atomically Thin Carbon Films. Science 306: 666-669.
10. Bablich A, Kataria S, Lemme MC (2016) Graphene and Two-Dimensional Materials for Optoelectronic Applications. Electronics 5:13.
11. Takeda K, Shiraishi K (1994) Theoretical possibility of stage corrugation in Si and Ge analogs of graphite. Phys Rev B 50: 14916-14922.
12. Guzman-Verri GG, Lew Yan Voon LC (2007) Electronic structure of silicon-based nanostructures. Phys Rev B 76: 075131.
13. Lalmi B, Oughaddou H, Enriquez H, Kara A, Vizzini S, et al. (2010) Epitaxial growth of a silicene sheet. Appl Phys Lett 97: 223109.
14. De Padova P, Quaresima C, Ottaviani C, Sheverdyaeva PM, Moras P, et al. (2010) Evidence of graphene-like electronic signature in silicene nanoribbons. Appl Phys Lett 96: 261905.
15. Vogt P, De Padova P, Quaresima C, Avila J, Frantzeskakis E, et al. (2012) Silicene: Compelling Experimental Evidence for Graphene-like Two-Dimensional Silicon. Phys Rev Lett 108: 155501.
16. Dávila ME, Xian L, Cahangirov S, Rubio A, Le Lay G (2014) Germanene: a novel two-dimensional germanium allotrope akin to graphene and silicone. New J Phys 16: 095002.
17. Khandelwal A, Mani K, Karigerasi MH, Lahiri I (2017) Phosphorene - The two-dimensional black phosphorous: Properties, synthesis and applications. Materials Science and Engineering B 221: 17.
18. Umrao S, Nirala NR, Khandelwal G, KumarV (2018) Chapter - Synthesis and Characterization of Phosphorene: A Novel 2D Material, Nanomaterials: Biomedical, Environmental, and Engineering Applications 2018: 61-92.
19. Zhu F, Chen W, Xu Y, Gao C, Gan D, et al. (2015) Epitaxial Growth of Two-Dimensional Stanene. Nature Materials 14: 1020.
20. Engler M, Lesniak C, Damasch R, Ruisinger B, Eichler J (2007) Hexagonal Boron Nitride (h-BN): Applications from Metallurgy to Cosmetics. Ceramic Forum International 84: E49.
21. Wang QH, Kalantar-zadeh K, Kis A, Coleman J, Strano MS (2012) Electronics and Optoelectronics of Two-Dimensional Transition Metal Dichalcogenides (TMDs). Nature Nanotechnology 7: 699-712.
22. Stokbro K, Petersen DE, Smidstrup S, Blom A, Ipsen M, et al. (2010) Semi empirical model for nanoscale device simulations. Phys Rev B 82: 075420.
23. Kienle D, Cerda JI, Ghosh AW (2006) Extended Hückel theory for band structure, chemistry, and transport. I. Carbon Nanotubes. J App Phys 100: 043714.
24. Huisman EH, Guédon CM, van Wees BJ, Van der Molen SJ (2009) Interpretation of transition voltage spectroscopy. Nano Lett. 9: 3909-3913.
25. Araidai M, Tsukada M (2010) Theoretical calculations of electron transport in molecular junctions: Inflection behavior in Fowler-Nordheim plot and its origin. Phys Rev B 81: 235114.
26. Forbes RG (2009) Use of Millikan-Lauritsen plots, rather than Fowler-Nordheim plots, to analyze field emission current-voltage data. J Appl Phys 150: 114313.
27. Xue, Y, Datta S, Ratner MA (2002) First-principles based matrix Green's function approach to molecular electronic devices: general formalism. Chemical Physics 281: 151-170.
28. Tian W, Datta S, Hong S, Reifenberger R, Henderson J, Kubiak CP (1998) Conductance spectra of molecular wires. J Chem Phys 109: 2874.

29. Di Ventra M (2008) Electrical Transport in Nanoscale System. Cambridge University Press. Pg No: 1-476.

30. PerdewJP, ZungerA (1981) Self-interaction correction to density-functional approximations for many-electron systems. Phys Rev B 23: 5048.

31. Cuevas JC, Scheer E (2010) Molecular Electronics: An Introduction to Theory and Experiment. World Scientific in Nanoscience and Nanotechnology, World Scientific Publishing Co. Pte. Ltd. Pg No: 1-703.

32. Zimbovskaya NA (2013) Transport Properties of Molecular Junctions. Springer New York. Pg No: 1-338.

33. Raza H (2012) Graphene Nanoelectronics: Metrology, Synthesis, Properties and Applications. Springer Press. Pg No: 1-587.

34. Landauer R (1957) Spatial Variation of Currents and Fields Due to Localized Scatterers in Metallic Conduction. IBM J Res Dev 1: 223.

35. Buttiker M (1986) Four-Terminal Phase-Coherent Conductance. Phys Rev Lett 57: 1761.

36. Wu CS e Chai JD (2015) Electronic Properties of Zigzag Graphene Nanoribbons Studied by TAO-DFT. J Chem Theor and Comput 11: 2003-2011.

37. Yao Y, Liu A, Bai J, Zhang X, Wang R (2016) Electronic Structures of Silicene Nanoribbons: Two-Edge-Chemistry Modification and First-Principles Study. Nanoscale Res Lett 11: 371.

38. Tao L, Cinquanta E, Chiappe D, Grazianetti C, Fanciulli M, et al. (2015) Silicene field-effect transistors operating at room temperature. Nat Nanotechnol 10: 227.

39. Aleixo VFP, Silva Jr. CAB, Del Nero J (2014) Molecular Electronic Junction Composed by C_{60} as Spacer and Four Terminals Formed by Acceptors Group: Transition-Voltage Spectroscopy. J Comput and Theor Nanosc 11: 637-641.

40. Tavares SCC, Conde-de-Sousa GT, Sousa MES, Aleixo VFP, Del Nero J (2014) Electrical Signature of Graphene and Dendrimer Nanoantennas. Comput Theor Nanosci 11: 1899.